

# Synthesis and Characterization of a Purely Random Thermotropic Terpolymer Based upon *p*-Acetoxybenzoic Acid, Hydroquinone Diacetate, and Azelaic Acid

John D. Carter

Corporate Research Division, The Goodyear Tire & Rubber Company, Akron, Ohio 44305

Received January 2, 1991; Revised Manuscript Received April 30, 1991

**ABSTRACT:** A purely random main-chain thermotropic polyester analogous to that obtained by polymerizing 4'-acetoxyphenyl 4-acetoxybenzoate and azelaic acid was synthesized by the terpolymerization of *p*-acetoxybenzoic acid, hydroquinone diacetate, and azelaic acid. Differential scanning calorimetry (DSC), solution viscosity, optical polarizing microscopy, carbon-13 nuclear magnetic resonance (<sup>13</sup>C NMR), and wide-angle X-ray diffraction (WAXD) measurements were used to characterize the polymer. <sup>13</sup>C NMR measurements showed a higher degree of randomness for the polymer obtained by this three-monomer method than for the random polymer obtained by the previously reported two-monomer method. DSC analysis of low molecular weight polymer (IhV < 0.30) revealed two thermal transitions associated with the crystalline- to nematic-phase transition. As the molecular weight of the polymer was increased, a third transition became apparent. This third transition increased in intensity with increasing IhV and was shown by WAXD measurements to be a transition other than the crystal-nematic transition, which has been hypothesized for similar systems.

## Introduction

A frequently presented concept for main-chain thermotropic liquid-crystalline polymers (LCPs) involves regular sequencing of uniform rigid and flexible segments of the polymer chain. A well-defined liquid-crystalline mesophase is obtained where such regular structure exists; i.e., one usually observes both well-defined crystalline to mesophase and mesophase to isotropic transitions. This perfectly alternating molecular arrangement is shown in the work of Meurisse et al.<sup>1</sup> These workers reacted the dimethyl ester of 4,4'-dicarboxybiphenyl with various aliphatic diols to achieve perfectly alternating sequences of rigid and flexible segments. Likewise, Krigbaum et al.<sup>2</sup> reacted 4,4'-diacetoxybiphenyl with various aliphatic diacids to arrive at similar ordered structures.

Since 4,4'-disubstituted phenyl benzoates are well-known<sup>3</sup> for their mesogenic activity, it would appear that the reaction of 4'-acetoxyphenyl 4-diacetoxybenzoates with aliphatic diacids would yield these regularly alternating thermotropic LCPs. Strzelecki and Liebert<sup>4</sup> carried out this reaction scheme with a homologous series of aliphatic diacids and obtained polymers that they perceived to consist of the 4,4'-disubstituted phenyl benzoate mesogen alternating with aliphatic flexible spacers.

Moore and Stupp<sup>5</sup> reacted pimelic acid with 4'-acetoxyphenyl 4-acetoxybenzoate to show that this two-monomer synthetic scheme produces a polymer with a randomized structure since the ester bond joining the phenyl rings of the phenyl benzoate mesogen readily undergoes transesterification during synthesis. The phenyl-phenyl bond of the biphenyl mesogen is obviously not subject to this problem.

Martin and Stupp<sup>6</sup> devised a synthetic scheme to prevent the randomization of the ester linkage between the phenyl moieties and compared the resulting regular polymer with the random polymer. That work demonstrated the effect of structural randomness on mesophase properties, particularly the loss of the well-defined mesophase-to-isotropic transition when structural randomness prevails.

Krigbaum et al.<sup>7</sup> prepared ordered structures by reacting 4'-hydroxyphenyl 4-hydroxybenzoate with the diacid chlorides of aliphatic diacids under mild solution conditions. This technique prevented the phenyl-phenyl ester

bond from scrambling but produced a regular placement of the mesogenic moieties within the backbone.

This work reports the synthesis and characterization of a totally random analogue of the polymers described in the above references. A purely random system should result from the terpolymerization of *p*-acetoxybenzoic acid (ABA), the diacetate of hydroquinone (HQDA) and azelaic acid (AZ). The polymer structure is represented in Figure 1 according to the convention of Moore and Stupp.<sup>5</sup> The use of AZ allows for comparison of both the corresponding polymer synthesized by Krigbaum et al.,<sup>7</sup> using the two-monomer method of Strzelecki and Liebert, and the corresponding regular alternating polymer.

## Experimental Section

**I. Synthesis. a. Materials.** ABA (National Starch), HQDA (Kodak), AZ (Emery), and sodium acetate catalyst (Mallinckrodt) were all of polymerization grade and were used as received.

**b. Apparatus.** The polymers were synthesized in a glass reactor fitted with a mechanical stirrer, a nitrogen inlet valve, and a distillation column. The distillation column was equipped with a vacuum takeoff. The reactor was submerged in an electrostatically heated oil bath whose temperature was monitored by a thermocouple that signaled a proportioning controller.

**c. Procedures.** The reaction vessel was charged with the monomers and catalyst, purged with nitrogen, heated to 130 °C, and maintained for 0.5 h under a nitrogen atmosphere. The temperature was raised to 250 °C and maintained until 80% of the theoretical acetic acid was distilled off. The temperature was then raised to 290 °C and vacuum pull down was immediately begun. A vacuum of 0.5 Torr was established over a 0.5-h period. After an additional 0.5 h the polymer was discharged.

The polymer was synthesized from essentially equal molar concentrations of ABA, HQDA, and AZ. HQDA was charged in slight excess since it was found that a certain amount sublimated from the monomer melt during polymerization. The HQDA molar ratio was therefore adjusted to yield optimum inherent viscosities (IhVs). Table I shows HQDA/AZ molar feed ratios together with resulting IhVs. Highest IhVs were obtained with 2% molar excess HQDA. The catalyst charge was 0.6 ppt based on the expected final polymer weight.

**II. Characterization.** Inherent viscosities were measured in tetrachloroethane/phenol (60/40) solutions. Differential scanning calorimetry (DSC) measurements were made on a Perkin-Elmer 7 Series instrument. The instrument was calibrated with an indium standard. Carbon-13 nuclear magnetic resonance

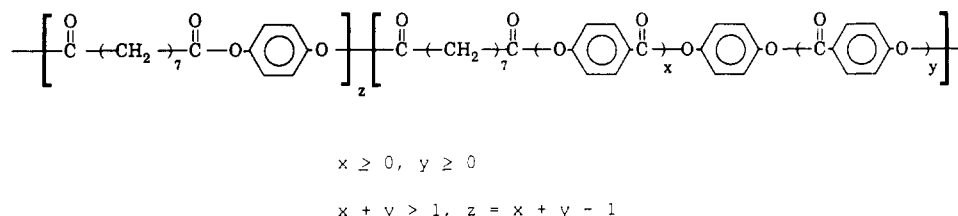


**Figure 1.** Structure of random liquid-crystalline terpolyester based on *p*-acetoxybenzoic acid, hydroquinone diacetate, and azelaic acid.

**Table I**  
Hydroquinone Diacetate/Azelaic Acid Molar Feed Ratios  
with Corresponding Inherent Viscosities

HQDA/AZ	IhV	HQDA/AZ	IhV
1.00	0.43	1.02	0.80
1.01	0.54	1.03	0.60

( $^{13}\text{C}$  NMR) measurements were made at 75 Hz with a Varian XL-300 in deuterated chloroform/trifluoroacetic acid solvent (90/10). The chemical shifts were recorded relative to the central peak of the chloroform triplet (77 ppm vs  $\text{SiMe}_4$ ). Optical textures were viewed with a Nikon Optiphot polarizing microscope in conjunction with a Mettler FP5 hot stage. Wide-angle X-ray diffraction (WAXD) patterns were obtained with a Rigaku DMAX IIA instrument ( $\text{Cu K}\alpha$  radiation.) A thin, narrow film of sample was placed in an aluminum foil support to provide mechanical integrity to the sample at high temperature. This was mounted in a Rigaku sample holder (CN2421A1), which is equipped (by Rigaku) with electric heating elements. This device was then mounted on a Rigaku fiber attachment device (CN2411B1). Temperature was monitored by a thermocouple with a cold junction. The sample to film distance was 78.5 mm.

## Results and Discussion

**I. Structural Consideration.**  $^{13}\text{C}$  NMR was used to examine the composition of the polymer. A random structure was expected to show four signals in the region of 160–180 ppm, representing four different carbonyls, as demonstrated by Moore and Stupp.<sup>5</sup> A  $^{13}\text{C}$  spectrum of the polymer synthesized by the three-monomer method, together with the signal assignments, is shown in Figure 2. Assignments were made on the basis of the model work of Moore and Stupp.<sup>5</sup> The observed signals are slightly shifted downfield relative to those reported by Moore and Stupp. This observed shift is probably due to different solvent systems.

Table II shows the composition and number-average sequence length of oxybenzoate units for two polymers of varying IhV. There are some differences in structural unit composition between the polymer synthesized by this three-monomer method vs that of the two-monomer method of Strzelecki and Liebert. The polymer resulting from this work has essentially equal molar ratios of the three structural units contained within the polymer. For the two-monomer method with pimelic acid as the spacer, Moore and Stupp reported that both pimelate and oxybenzoate moieties were lost by sublimation during polymer synthesis. This loss was compensated for by adding excess diacid to the feed charges.<sup>5</sup> For the three-monomer method used here, little AZ was lost; most of the sublimate was HQDA, and this was compensated for in the feed charges as shown in Table I. The balance between the AZ and HQ moieties found in the polymer is the expected 1/1 ratio (Table II). The number-average sequence length of oxybenzoate units ( $\bar{l}_{ob}$ ) is the expected length (1.5) for a completely random terpolymer where equal fractions of the monomers are present.<sup>5</sup>

**II. Thermal Analysis.** Thermal properties of the random terpolyester as a function of IhV were examined

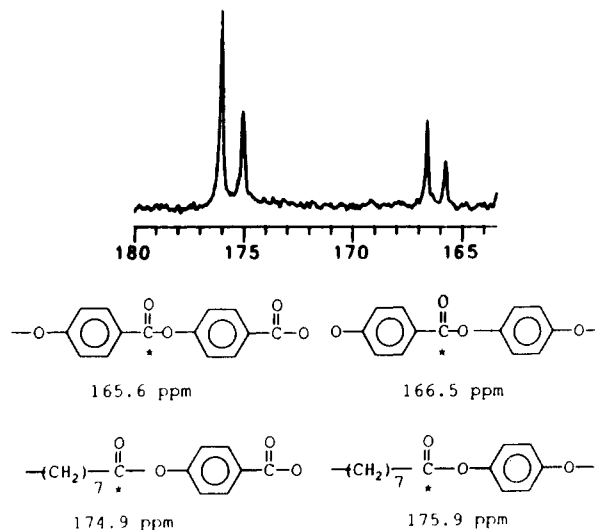


**Figure 2.** Partial  $^{13}\text{C}$  NMR spectrum and signal assignments for random thermotropic terpolyester.

**Table II**  
Terpolymer Composition and Oxybenzoate Sequence  
Length for the Terpolymer of *p*-ABA, HQDA, and AZ  
Determined from  $^{13}\text{C}$  NMR

polymer IhV	mol %			$\bar{l}_{ob}$
	dioxyphenyl	oxybenzoate	azelaate	
0.46	0.34	0.32	0.34	1.5
0.75	0.33	0.34	0.33	1.5

by DSC. In the DSC thermograms shown in Figure 3, the second and third scans are shown. The first scan was not considered since one sometimes observes artifacts due to coalescence of the sample. A third scan is included to demonstrate the general reproducibility of the transitions shown in the second scan.

On the low end of the IhV scale ( $\text{IhV} = 0.27$ ), two endotherms were usually observed ( $T_1$  and  $T_2$ ). On heatup (Figure 3a), these appeared extremely close to one another. Sometimes only one peak was observed on heating the very low IhV polymer. According to polarizing light microscopy and wide-angle X-ray diffraction, these endotherms (or endotherm, if only one appeared) are associated with a crystalline to nematic transition. On further heating, onset of a biphasic morphology was observed via the polarizing microscope beginning at  $\sim 220^\circ\text{C}$ . This transition was too broad and too low in energy to be readily detected by DSC. On cooling, DSC consistently revealed two transitions.

As the molecular weight of the polymer was increased ( $\text{IhV} = 0.52$ , Figure 3b), a higher temperature transition ( $T_3$ ) appeared as a small tail to the endotherm associated with  $T_2$  ( $T_1$  in this case did not appear on heatup). It was uncertain if  $T_3$  represented a crystalline to nematic transition or a mesophase to mesophase transition. It was thought that this transition might represent a mesophase to mesophase transition since  $T_3$  was absent in the lower

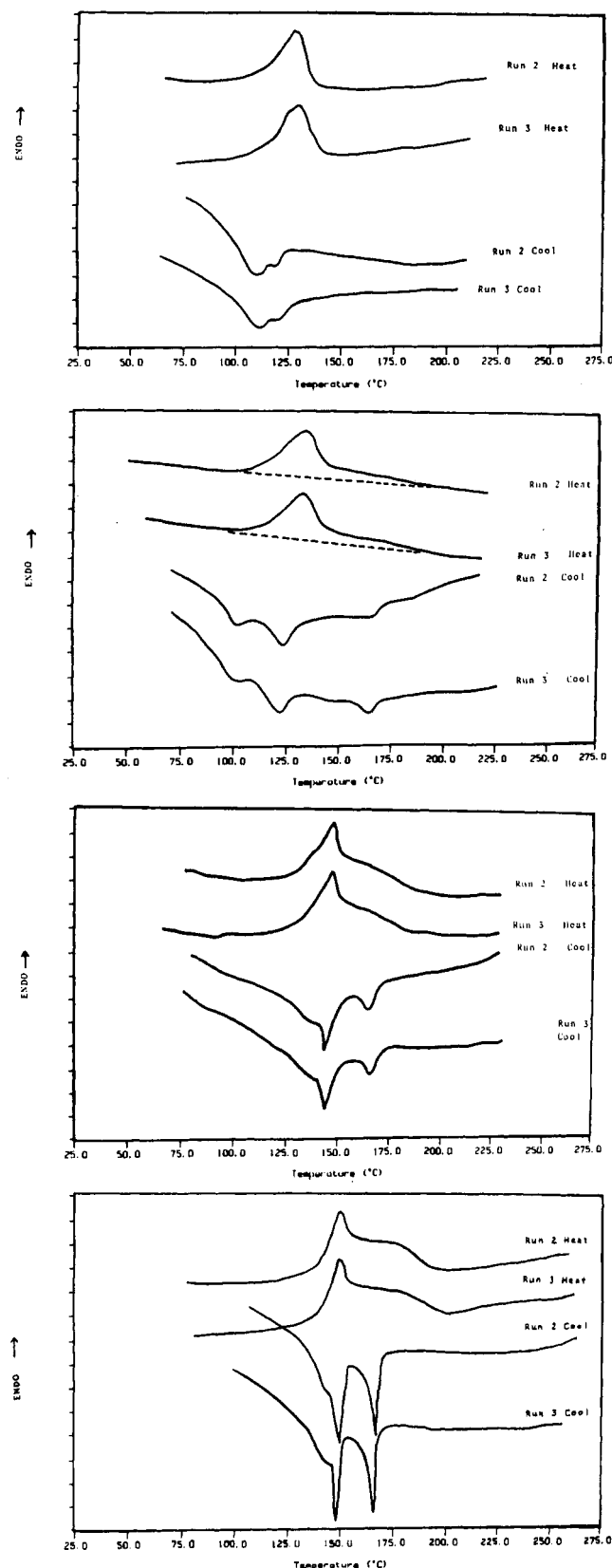


Figure 3. DSC thermograms for random thermotropic polyester of (from top to bottom) (a)  $IhV = 0.27$ , (b)  $IhV = 0.52$ , (c)  $IhV = 0.70$ , and (d)  $IhV = 1.1$ .

molecular weight polymer. On cooling,  $T_1$ ,  $T_2$ , and  $T_3$  were all apparent.

As the molecular weight of the polymer was further increased ( $IhV = 0.70$ , Figure 3c),  $T_1$  and  $T_2$  shifted toward higher temperatures.  $T_3$  on the heating scan became more apparent, although it still appeared as a broad, smeared-

Table III  
Thermal Analysis Summary

sample	$IhV$ , dL/g	transtn temp, <sup>a</sup> °C			$\Delta H$ (total transtns), J/g	approx onset of biphasic, <sup>d</sup> °C
		$T_1$	$T_2$	$T_3$		
(A) DSC Heating Scan (10 °C min)						
A	0.27	129	131	<i>a</i>	16	220
B	0.52	<i>a</i>	133	<i>b</i>		220
C	0.70	133	146	165	19	230
D	0.77	<i>a</i>	147 <sup>c</sup>	<i>b</i>	20	260
E	1.11	145 <sup>c</sup>	150	<i>b</i>	19	270
(B) DSC Cooling Scan (10 °C min)						
A	0.27	109	120	<i>a</i>	16	
B	0.52	101	122	166		
C	0.70	135	145	166	19	
D	0.77	138	146	169	20	
E	1.11	140	149	167	19	

<sup>a</sup> Not observed. <sup>b</sup> Observed but too broad to assign a transition temperature. <sup>c</sup> Taken from thermogram not shown. <sup>d</sup> Temperature taken from optical polarizing microscope.

Table IV  
Thermal Transitions in Polymer D (Table III) Annealed at 120 °C for 24 h

thermogram	mode	transition temp, <sup>a</sup> °C			$\Delta H$ (total transtn), J/g
		$T_1$	$T_2$	$T_3$	
a	heat original	140	147	<i>b</i>	24
b	cool	140	148	170	18
c	reheat	<i>a</i>	147	<i>b</i>	18

<sup>a</sup> Not observed. <sup>b</sup> Generally too broad to assign a single transition temperature.

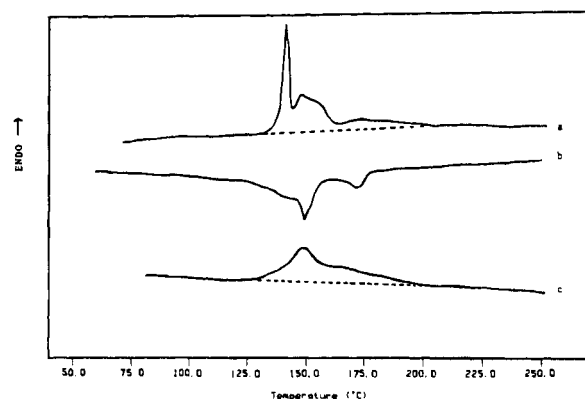
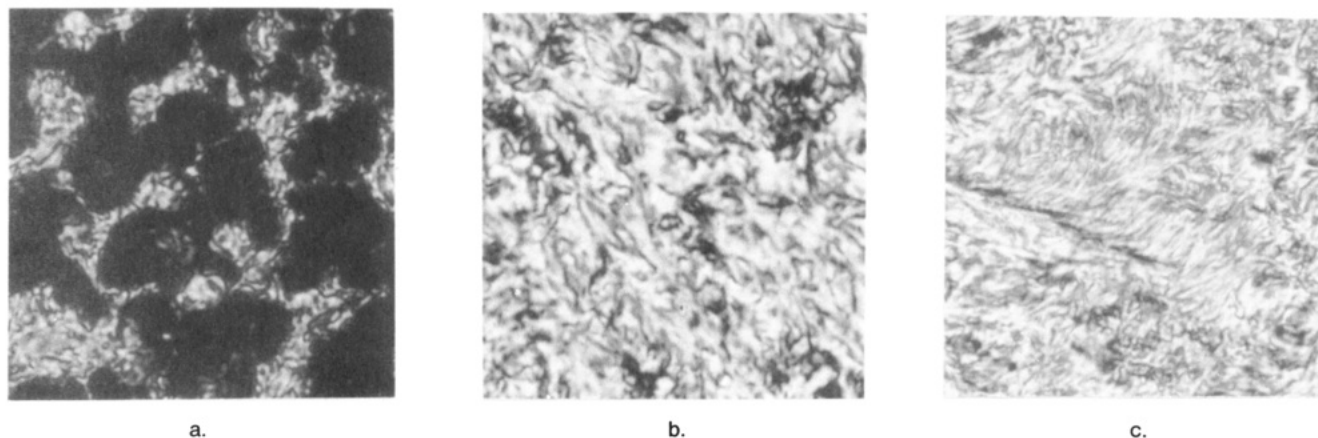


Figure 4. DSC thermograms for random thermotropic polyester of 0.77  $IhV$  (a) annealed at 120 °C for 24 h, (b) cooled from isotropic state, and (c) reheated.

out transition.  $T_3$ , upon cooling, appeared at essentially the same temperature as observed in the lower molecular weight sample.  $T_3$  in this higher molecular weight material had a higher enthalpy associated with it than that observed in the lower molecular weight sample.

A further increase in polymer  $IhV$  ( $IhV = 1.1$ , Figure 3d) revealed an even larger tail ( $T_3$ ) associated with  $T_2$ .  $T_2$  was again shifted to a slightly higher temperature.  $T_3$  increased in enthalpy relative to the lower  $IhV$   $T_3$  transition.  $T_3$ , however, shifted very little in temperature.

Table IIIA summarizes the thermal transitions observed on heating as a function of  $IhV$ .  $T_1$  was not always observed on heatup. When it was observed, it usually appeared as a small shoulder on  $T_2$ . Its appearance in the DSC heating scan may be related to sample history or heating rate. It often appeared when the heating rate was slowed, but this was not always reproducible. On the basis of these observations, it is hypothesized that  $T_1$  is a crystal to crystal transition.  $T_2$  always appeared as a fairly sharp transition,



**Figure 5.** Optical micrographs for polymer E (Table III). Key (from left to right): (a) 280 °C, (b) 200 °C cooled from isotropic state, (c) 160 °C cooled from isotropic state.

and it shifted to slightly higher temperatures with increasing molecular weight.  $T_3$  appeared as a large tail to  $T_2$ , and its energy increased with the IhV of the polymer. The enthalpy, as calculated from the sum of the transitions, was higher for the higher IhV samples, although there was no separation in enthalpy value for the samples with IhV in the 0.7–1.1 range.

Table IIIB summarizes the transitions observed on cooling as a function of IhV. Although  $T_1$  was sometimes difficult to see in the heating scan, it appeared consistently in the cooling scan. At low IhVs,  $T_1$  appeared to be of higher energy than  $T_2$ . As IhV increased,  $T_1$  became less dominant than  $T_2$ .  $T_3$  was absent in the low molecular weight sample.  $T_3$  appeared with increasing intensity as the IhV of the polymer increased. The temperature of  $T_3$  remained fairly consistent, while the temperature of  $T_2$  was observed to increase with increasing molecular weight. The total enthalpy of the transitions on cooling agreed with those obtained from the heating scan.

Polymer sample D from Table III was annealed at 120 °C for 24 h and the transitions were subsequently reexamined. The resulting thermograms are shown in Figure 4. In the initial heating scan (Figure 4a) an additional transition was observed. The well-defined endotherm appearing at 140 °C apparently corresponds to  $T_1$  observed previously in some of the lower molecular weight samples. The main endotherm appearing at 147 °C ( $T_2$ ) in the unannealed sample (see Table III) appears as the weaker transition in the annealed sample. The broad transition appearing as  $T_3$  in the unannealed sample appears resolved into two distinct transitions in the annealed sample. One of these is seen as a shoulder on  $T_2$  and the other as a very low energy and highly smeared out transition. The enthalpy of the total transitions, 24 J/g, is only slightly higher than that observed in the unannealed sample, 20 J/g. On cooldown from the isotropic state, the annealed polymer shows essentially the same thermal behavior previously observed in the nonannealed sample (Figure 4b). Reheating the sample shows again (Figure 4c) the same thermal behavior observed in the unannealed sample; i.e.,  $T_1$  is not observed and  $T_3$  is a broad smeared-out transition. The transition temperatures and enthalpy values for the thermograms of Figure 4 are given in Table IV.

**III. Optical Microscopy.** The multiple transitions occurring between 125 and 170 °C on the heat cycle were not readily detected by polarizing optical microscopy. The texture on heatup did not appreciably change before the onset of isotropization. It was, however, necessary to use the microscope for detection of the isotropization tem-

perature, since this transition did not appear in the DSC scan. Isotropization occurred over an approximate 70 °C temperature range. The approximate temperature of onset for the observed nematic–isotropic biphasic morphology is listed in Table IIIA for the varying molecular weight polymers. An optical micrograph (Figure 5a) of polymer E from Table III at 280 °C clearly shows regions of isotropic polymer (dark areas) alongside regions of polymer in a nematic mesophase. When the polymer was cooled to 200 °C from the isotropic state, it entered a nematic mesophase as shown in Figure 5b. Figure 5c shows the texture obtained at 160 °C after the polymer had gone through  $T_3$  on cooldown. This texture was obtained after ~16 h at 160 °C. It was not observed in short periods of time. On the basis of the thermal and optical results, it was suspected that  $T_3$  perhaps represented a mesophase to mesophase transition and not the crystalline to nematic transition that has been hypothesized for a similar and corresponding system.<sup>7</sup>

**IV. Wide-Angle X-ray Diffraction.** To further investigate the nature of  $T_3$ , WAXD measurements were made on the polymer by Dr. R. Thudium of Goodyear Research. Room-temperature measurements of polymer E from Table III revealed an intense crystalline peak with a spacing of 4.3 Å. A diffuse peak at a much lower angle was also observed. This low-angle diffuse scattering pattern is somewhat characteristic of molecular order found in nematic phases.<sup>8</sup> A diffraction measurement on an injection-molded sample of the polymer (Figure 6a) revealed splitting into arcs of this low-angle reflection indicative of chain orientation. This is strong evidence that the low-angle scattering is other than air scatter. Figure 6b shows the Laue photo at room temperature for an unoriented sample. The sample was heated to 200 °C and maintained at this temperature until complete loss of crystalline memory was achieved. The diffraction pattern at 200 °C (Figure 6c) appeared as one might expect for an amorphous morphology. This is presumably because of the low degree of ordering of the nematic mesophase in the absence of an ordering field as is the case here. (For a similar polymer, Liebert and co-workers<sup>2</sup> reported order parameters of only 0.5–0.6 for samples aligned in a magnetic field of 3 kG for 24 h.) However, on the basis of the optical birefringence and texture of the polymer at 200 °C (Figure 5b), it is reasonable to conclude that the polymer is in a nematic mesophase at this temperature. The temperature was then dropped to 160 °C. The polymer at this temperature has gone through  $T_3$  but has not yet gone through  $T_2$ . Figure 6d shows the Laue photo for the polymer in thermal equilibrium at 160 °C. The

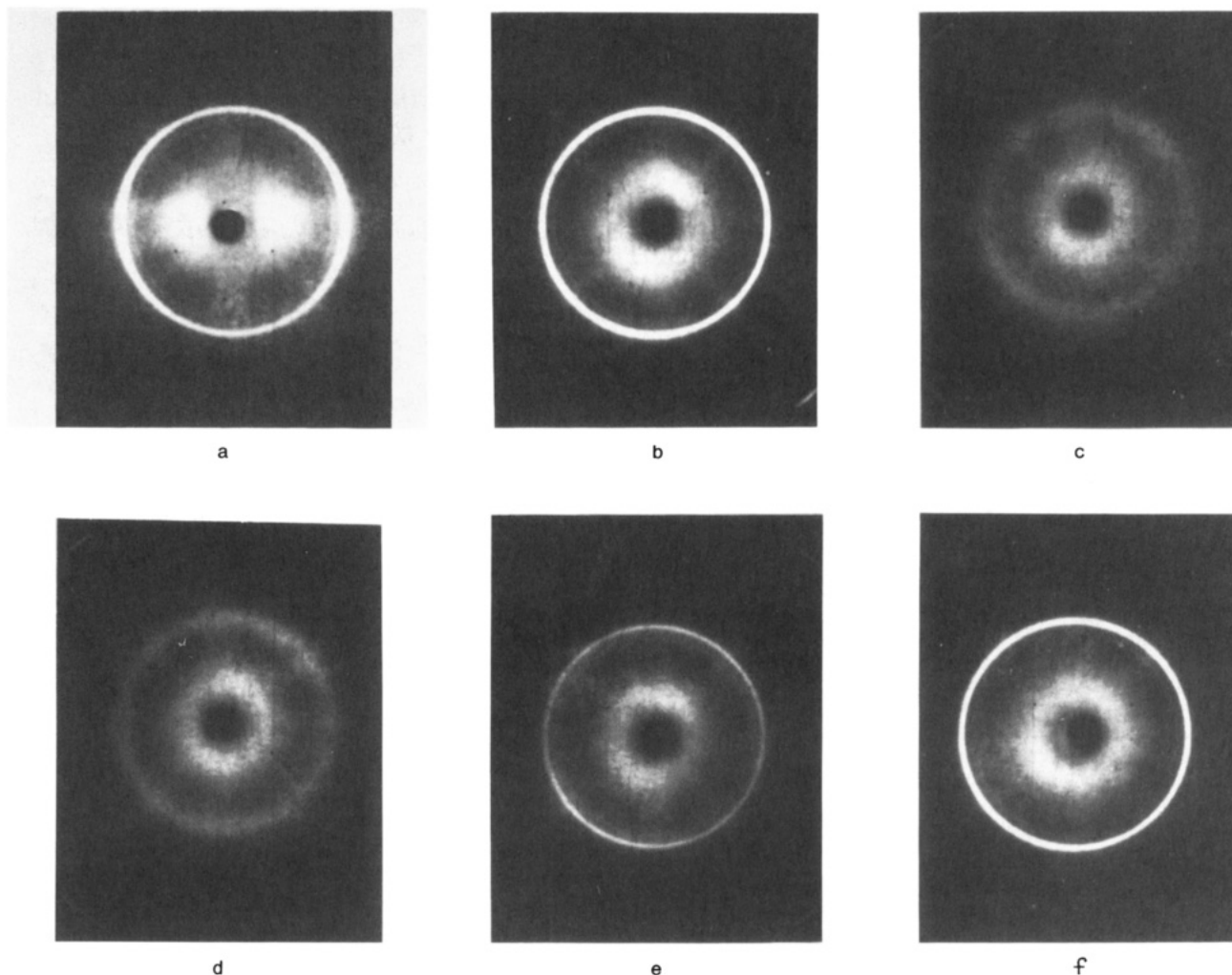


**Figure 6.** WAXD patterns for polymer E (Table III). Key (from left to right): (a) injection molded at room temperature, (b) room temperature, (c) 200 °C, (d) 160 °C on cooling, (e) 145°C on cooling, (f) room temperature on cooling.

absence of a sharp diffraction ring indicates that  $T_3$  is not a crystal-nematic transition. After cooling through  $T_2$ , the Laue photo reveals the sharp ring expected for a crystalline structure (Figure 6e). Further cooling through  $T_1$  (Figure 6f) reveals an even sharper diffraction ring, which supports the hypothesis that  $T_1$  is a crystal-crystal transition.

### Conclusions

While the WAXD measurements provide strong evidence that the high-temperature transition is not a crystalline transition, they do not allow for identification of the phase existing between  $T_2$  and  $T_3$  as hoped for. It has been shown that the existence of this phase is molecular weight dependent. It is probably not unique to the  $C_7$  aliphatic spacer, since Stupp and Martin<sup>8</sup> have reported in their polymer an unidentified transition occurring at  $\sim 160$  °C upon cooling. The existence of a smectic phase would account for their inability to orient this polymer in a magnetic field slightly below 160 °C even though the polymer is above the crystalline melting point at this temperature. Optical microscopy suggests that the phase in question might be a smectic phase; however, this cannot be concluded on basis of the microscopy evidence alone. The high-temperature X-ray technique used in this work is not amenable to annealing the sample for prolonged periods of time. Therefore, a sharpening of the low-angle X-ray reflection, indicative of a smectic phase, even if it existed, could probably not be

observed with the techniques available to us. It is hoped that further work will help to clarify the nature of this transition.

**Acknowledgment.** I express my thanks to Drs. R. Thudium and J. Visentainer of Goodyear Corporate Research Division for the WAXD and  $^{13}\text{C}$  NMR measurements, respectively. Discussion of X-ray analysis of liquid-crystalline polymers with Dr. Craig Burkhart was helpful. The Goodyear Tire & Rubber Co. is thanked for permission to publish this work.

### References and Notes

- (1) Meurisse, P.; Noel, C.; Monnerie, L.; Fayolle, B. *Br. Polym. J.* 1981, 13, 55.
- (2) Asran, J.; Toruimi, H.; Watanabe, J.; Krigbaum, W. R. *J. Polym. Sci., Polym. Phys. Ed.* 1983, 21, 1119.
- (3) Demus, D.; Demus, H.; Zashke, H. *Flussige Kristalle in Tabellen I*; VEB Beutscher Verlag fur Greinstoffindustrie: Leipzig, 1974.
- (4) Strzelecki, L.; Liebert, L. *Eur. Polym. J.* 1981, 17, 1271.
- (5) Moore, J. S.; Stupp, S. I. *Macromolecules* 1987, 20, 273.
- (6) Martin, P. G.; Stupp, S. I. *Macromolecules* 1988, 21, 1222.
- (7) Krigbaum, W. R.; Kotek, R.; Ishikawa, T.; Hakemi, H.; Preston, J. *Eur. Polym. J.* 1984, 20, 225.
- (8) Noel, C. In *Recent Advances in Liquid Crystalline Polymers*; Chopoy, L., Ed.; Elsevier: New York, 1985.
- (9) Liebert, L.; Strzelecki, L.; Van Luyen, D.; Levelut, A. *Eur. Polym. J.* 1981, 17, 71.